EFFECT OF BUBBLE INTERFACE POSITION ON PROPULSION AND ITS CONTROL FOR OSCILLATING-BUBBLE POWERED MICROSWIMMER

Fang-Wei Liu, Ye Zhan, and Sung Kwon Cho
University of Pittsburgh, Pittsburgh, USA

ABSTRACT

It has been previously reported that a gaseous bubble trapped in a one-end-open tube oscillates in the presence of acoustic wave and generates strong microstreaming flows and thus a propulsion force. The propulsion highly depends on the frequency and the voltage of the external acoustic wave. This paper presents a new discovery that the direction of this propulsion is dependent on the relative location of the bubble interface. The oscillating bubble propels forward when its interface stays deep inside the tube. On the contrary, the bubble propels in a reverse direction when its interface is at the exit of the tube. Learning from this phenomenon, we developed and introduced physical structures (necks) to precisely control the location of the bubble interface. As a result, the length and interface position of the bubble is more controllable, and the bubble oscillation and propulsion becomes more predictable and consistent.

INTRODUCTION

An acoustic wave induces oscillations in a gaseous bubble immersed in a liquid. In particular, when a bubble is confined by solid boundaries (e.g., bubble trapped in a one-end-open tube), the air-water interface near the tube opening oscillates back and forth and generates a non-zero time-averaged flow field in the surrounding, which is called microstreaming [1]. However, this flow is generated only when the inertia effect becomes significant. In other word, the oscillating Reynolds number (defined in Eq. (1)) should be high enough [2].

$$Re = \frac{2\rho R (2\pi f) a}{\mu} \qquad (1)$$

where ρ is the density of fluid, R is the equivalent radius of the tube, a is the amplitude of the interface oscillation, f is the frequency of the oscillation, and μ is the viscosity of the fluid. An easy way to reach high Re with a micro bubble is to increase the oscillating frequency f. This microstreaming flow in turn generates a net force on the bubble, resulting in bubble propulsion opposite to the streaming flow. This propulsion principle was first introduced by Dijkink *et al* [3], which is known as "acoustic scallop". Then, Feng *et al* adopted this principle in a microscale and developed microswimmers using the microfabrication technology [2]. Here, the swimmers were propelled uni-directionally (forward) only. In addition, they showed numerically and experimentally that the propulsion force is proportional to the oscillation amplitude and frequency. In general, the propulsion force reaches its maximum at the resonance frequency of the bubble. Later, this group further developed the microswimmer by adding the capability of 2-D steered propulsion [4]. The idea is to use multiple bubbles oriented in different directions. Of course, the individual bubbles are different in length and

thus resonate at different frequencies. This configuration allows for selectively activating the individual bubbles by changing the frequency. That is, if one may want to propel forward, the resonance frequency of the bubble, of which opening faces backward, should be selected, or vice versa. Similarly, if one may want to turn right, the bubble, of which opening faces left, should be resonated, or vice versa.
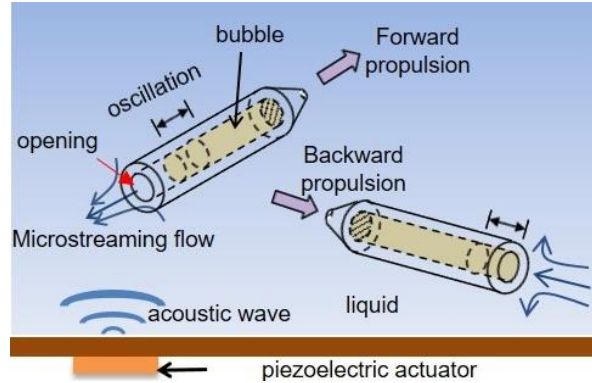

Figure 1: The microswimmer is powered by the gaseous bubble trapped inside. As the acoustic field applied, the bubble oscillates and generates a propulsion force forward or backward depending on the meniscus position.

The pre-requisite for this 2-D steering scheme is that the resonance frequencies among the individual bubbles should be clearly distinct and differentiable. The resonance behavior of the bubble oscillation is influenced by many parameters such as the bubble length, testing chamber, acoustic actuators, etc. Among them, the bubble length is critically important and potentially controllable. In the previous studies, the bubble length was roughly determined by the tube length. That is, when dried microtubes were submerged in water, air was trapped in the tube due to hydrophobicity of the tube inner surface. However, it showed a significant variation in the trapped bubble length. As a result, the bubbles showed inconsistent resonance behaviors and made 2-D steering more difficult. Therefore, the motivation of this work is to develop a method to control the length of trapped bubbles more precisely. The idea is to introduce a geometrical structure (like bottle neck) at the opening of the tube. The neck acts as an energy barrier (stopper) stopping water wetting right at the neck by re-directing the dominant interfacial tension [5]. As a result, the overall bubble length and interface position can be well fixed at a designed state, and the resonance behavior and propulsion will be more consistent since the bubble resonance highly depends on the bubble length.

In the meantime, while investigating the location of the bubble interface and bubble length, a remarkable phenomenon was discovered that the direction of propulsion depends on the position of the interface. When

the bubble interface is placed deep inside the microtube, the swimmer propels forward. While the interface is located at the exit of the tube, the propulsion direction is reversed. In the previous studies, it has been recognized that the propulsion direction was always opposite to the opening of the tube since it generated microstreaming flow near the tube opening was *outgoing*. Here, however, the propulsion direction was found reversible, which depends on the relative position of the bubble interface to the tube opening. To the authors' best knowledge, this finding has never been reported before.

EXPERIMENTAL
Study of Propulsion Reversal
To examine propulsion reversal, a commercially available a micro glass capillary with inner diameter of 300 μm, outer diameter of 600 μm, length at 1200 μm was used. The one end of the tube was blocked by thermal heating. To make the inner and outer surface hydrophobic, the tube was immersed in a Teflon solution and dried. This swimmer was tested in two different fluids, pure water (viscosity: 1.0×10^{-3} Pa·s) and water/glycerin mixture (viscosity: 3.5×10^{-3} Pa·s) to simulate the blood viscosity. The experimental setup included an acrylic tank filled with the fluid mentioned above, a piezoelectric disk of the diameter of 35 mm glued on the wall of the tank, a function generator with an amplifier connected to the piezoelectric disk to generate sinusoidal acoustic waves. The propulsion speed of the micro-capillary swimmer was measured at different voltages applied to the piezoelectric actuator, which are proportional to the amplitude of oscillation.

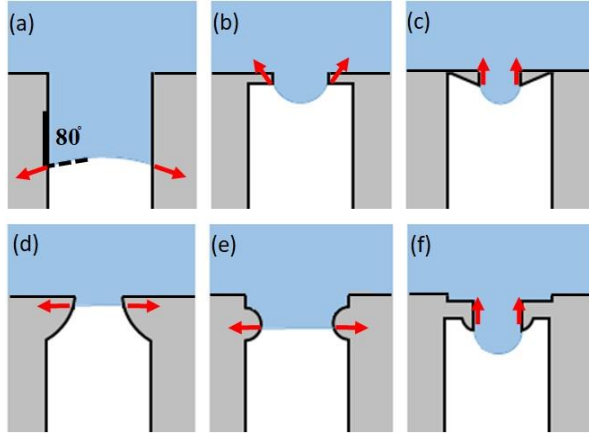### Controlling of Interface Position

Figure 2: Introduction of necks to the tube opening to pin the interface: (a) No neck; (b-f) Different designs of necks. The grey area indicates the wall of microtubes, the white region is the air bubble trapped inside the tube, and the blue part is water. The red arrows indicate the interfacial tension.

The microswimmer was fabricated through standard micro photolithography. The parylene structure by the CVD (chemical vapor deposition) process is a backbone of the microswimmer. First, a layer of 7-μm thick parylene was deposited on a silicon wafer for the bottom layer of microtubes, followed by a sacrificial layer of photoresist to define the rectangular cavity of microtubes with the width of 80 μm, height of 45 μm, and length ranging from 500-2000 μm. Then, another layer of 7 μm parylene was deposited for the top and wall of the microtube. Reactive ion etching (RIE) was used to open the microtubes exit and dice the microswimmer out. Afterward, an acetone solution removed the sacrificial photoresist layer and lifted off the swimmer from the substrate. Various designs of the neck were incorporated to the tube opening to fix the interface position, as shown in Fig. 2. All of them have the width of 40 μm and are located 50 μm inside from the tube exit edge. To observe the interface pinning at the necks, the microswimmer was placed at the depth of 3 cm in the DI water testing tank. The frequency applied to the piezoelectric disk was swept from 1.5 to 15 kHz with the voltages ranging from 150 V to 250 V. The amplitudes of bubble oscillation were captured using a high-speed camera.

RESULTS AND DISCUSSIONS
Study of Propulsion Reversal
The effect of the interface position on the propulsion direction is shown in Fig. 3, which are sequential snapshots during the micro-capillary swimmer propelled under the same acoustic field. In Fig. 3(a), the position of the bubble interface is located inside of the tube; while in Fig. 3(b) most part of the interface is outside of the tube. The three-phase contact line is pinned at the edge of the tube exit. The former (Fig. 3(a)) shows that the microstreaming flow was in the outgoing direction from the opening of the tube, thus generating a forward propulsion to the swimmer. On the contrary, the latter (Fig. 3(b)) showed a propulsion reversal. Accordingly, the streaming flows are also reversed.
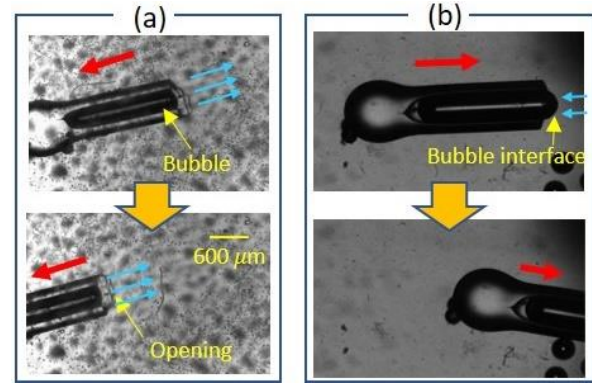

Figure 3: (a) Forward propulsion and (b) Backward Propulsion of capillary tube swimmer in the fluid of the blood viscosity (3.7 kHz). The position of gas-liquid (bubble) interface relative to the tube opening affects the propulsion direction. The red arrows denote the propulsion direction, and the blue arrows show the direction of microstreaming flow

Subsequently, the micro-capillary swimmers with the bubble interface inside or outside the tube were activated by different voltages in two fluids, pure water and mixture of water and glycerin (similar viscosity of blood). In both

fluids (Fig. 4), the propulsion speed increases as the voltage is increased. This trend can be confirmed by the previously derived equation describing the propulsion force on an oscillating bubble trapped in a tube [2]:

$$F \cong 0.8\rho A(af)^2 \qquad (2)$$

where ρ is the density of fluid, A is the cross-section area of the tube, a is the amplitude of the interface oscillation, and f is the frequency of the oscillation. Here, the increasing voltage directly raises the amplitude of the bubble oscillation, thus generating higher force to propel the swimmer faster. However, in the high viscosity solution (water/glycerin mixture), the drag force is higher than that in the low viscosity fluid, as the swimming speed (Fig. 4(b)) is overall slower than that in Fig. 4(a). Interestingly, a distinct difference in the direction of propulsion for two bubble interface configurations, inside or outside of the tube, appears in both liquids. The propulsion reversal occurs in a particular window of the input voltage from 10V to 30V when the interface is located outside the tube. More interestingly, when the voltage is around 75 V, this flow reversal, although weak, occurs again even with the interface inside the tube (Fig. 4(a)). This seems that some part of the interface is extended outside the tube exit due to large oscillation. Based on the preliminary flow visualizations (not shown here), the flow reversal accompanies reversals in the microstreaming flow. However, a further investigation is required on why and in what condition this reversal occurs.
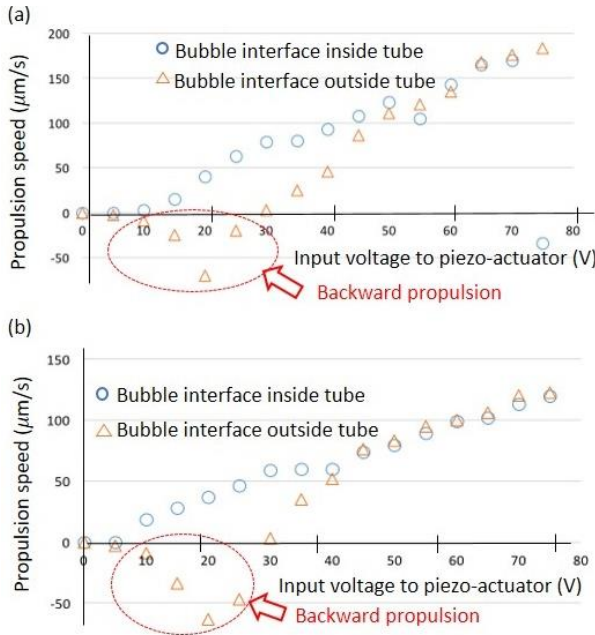

Figure 4: Propulsion speed of capillary tube swimmer vs. input voltage to piezo-actuator; (a) propulsion in water (viscosity 1.0 × 10-3 Pa ·s), and (b) propulsion in water + glycerin (viscosity 3.5 × 10-3 Pa · s, similar to blood viscosity).

Controlling of Interface Position

As the microfabricated parylene-based microswimmer was immersed in water, air bubbles were automatically trapped in the hollow microtubes. The locations of the air-water interface with and without the neck designs were observed under an optical microscope, as shown in Figs. 5(a) and (b). Without the neck at the tube exit, the straight inner wall of the microtube results in a concave interface, due to the intrinsic contact angle of about 80°, as illustrated in Fig. 2(a). As a consequence, the interfacial tension points inward and drags water into the microtubes. However, owing to the non-uniform roughness of the inner wall of microtubes, the locations of interface were randomly positioned over microtubes, thus resulting in variations in the lengths of bubbles even under the same fabrication batch and submerging condition. This variation in the bubble length will lead to difficulties in selectively actuating bubbles for steering propulsion. On the contrary, for 5 different structures of neck on the same microswimmer in Fig. 5(b) from left to right that correspond to the designs in Fig. 2(b-f), all the interfaces were well pinned at the location of bottle necks. It shows that the necks successfully hold the air-water interface by changing the direction of interfacial tension. Afterward, the microswimmer was actuated by applying an acoustic wave at 6.3 kHz and 150V. Sequential images were taken over a period of 5 second, and the comparison between the initial and final positions is shown in Fig. 5 (c). The microswimmer was able to propel over a few hundred micrometers while all the interfaces were pinned at the necks; however, the route was not completely straight. This may be due to the non-uniform friction from the bottom of the tank.
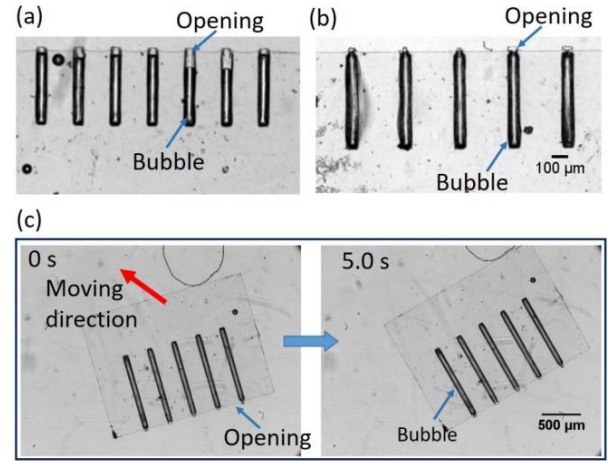

Figure 5: Bubble trapping (a) without and (b) with the neck structure in the tube opening. (c) The microswimmer with necks in the tube openings is propelled at 6.3 kHz and 150 V.

The behavior of bubble oscillation was verified by measuring the oscillation amplitudes at the same voltage but different frequencies. By sweeping the frequency of the external acoustic field from 1.5 to 15 kHz, the spectrum of bubble oscillation was measured, as shown in Fig. 6. Regardless of the length, every bubble had a distinct peak at 4.9 kHz. It is inferred that 4.9 kHz is the natural frequency of the entire system, the tank with the water, at

which the energy transmits most efficiently to the bubble, thus causing a local maximum. Therefore, this peak will be excluded from the discussion of the bubble behavior responding to the external acoustic field later. In Fig. 6(a), without the neck structure, two bubbles trapped in microtubes of the same dimensions had different lengths, 300 μm and 700 μm. They were on the same microswimmer and examined under the same frequency range simultaneously. It shows that the long bubble is more active in low frequency region and has the natural frequency at 8 kHz; on the other hand, the short bubble resonates at 12.7 kHz and does not noticeably responded in low frequency range. In Fig. 6(b), two bubbles, that have the same length at 1200 μm due to the neck structures, are trapped on the same microswimmer. Due to the same lengths, they show the almost identical response to the frequency over the entire spectrum in Fig. 6(b). They also have the same natural frequencies at 6.3 kHz.
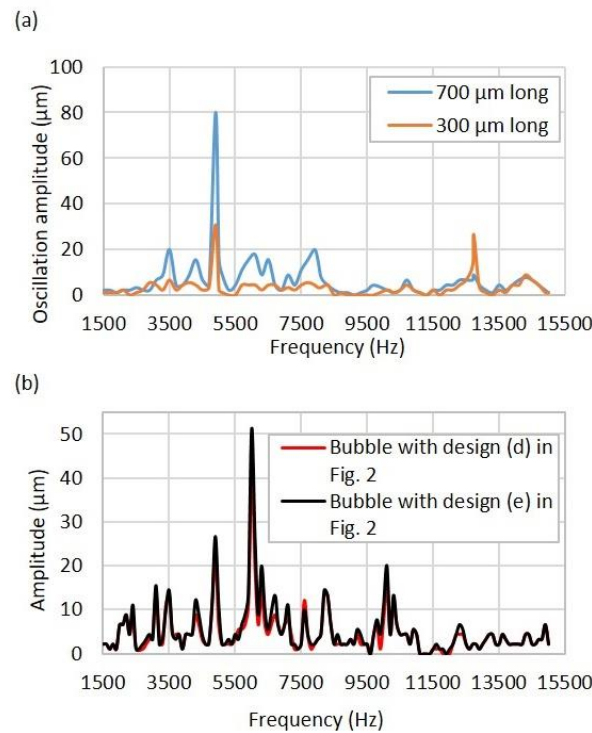
(a)

(b)

Fig. 6. Spectra of the amplitude of bubble oscillation under different frequencies. (a) Two bubbles (700 and 300 μm long) trapped without the neck are on the same chip, and show different oscillation spectra. (b) Two bubbles are trapped in the same length (1200 μm) due to the neck in the tube opening (designs (d) and (e) in Fig. 2), and show almost identical oscillation spectra.

CONCLUSION

Acoustically oscillating bubbles have been widely studied as they generate strong propulsion forces via microstreaming in the microfluidic environment. In this article, a novel discovery in the microstreaming flow is presented that the propulsion force depends on the relative location of air-bubble interface. More specifically, when the interface is located at the exit, a reversal in the propulsion direction occurs. This discovery provides more options in controlling the propulsion of the bubble-powered microswimmer. In addition, to do precise manipulations and generate complex movements of microswimmers, it is essential to maintain the bubble size consistent and reproducible. By introducing an extra geometrical structure (neck) to pin the interface, successful positioning the interface at desired position was achieved resulting in a consistent bubble length. This outcome provides a predictable behavior to bubble oscillation which is advantageous for precise and repeatable performance of the microswimmer.

REFERENCES
[1]   A. Hashmi, G. Yu, M. Reilly-Collette, G. Heiman, and J. Xu, "Oscillating bubbles: a versatile tool for lab on a chip applications," *Lab Chip,* vol. 12, p. 12, 2012.
[2]   J. Feng, J. Yuan, and S. K. Cho, "Micropropulsion by an acoustic bubble for navigating microfluidic spaces," *Lab Chip,* vol. 15, p. 9, 2015.
[3]   R. J. Dijkink, J. P. van der Dennen, C. D. Ohl, and A. Prosperetti, "The 'acoustic scallop': a bubble-powered actuator," *J. Micromech. Microeng.,* vol. 16, p. 7, 2006.
[4]   J. Feng, J. Yuan, and S. K. Cho, "2-D steering and propelling of acoustic bubble powered microswimmers," *Lab Chip,* vol. 16, p. 9, 2016.
[5]   T. L. Liu and C.-J. C. Kim, "Turning a surface superrepellent even to completely wetting liquids," *Science,* vol. 346, p. 5, 2014.

CONTACT
S.K. Cho, tel: +1-412-624-9798; skcho@pitt.edu